Green Chemistry

PAPER

View Article Online
View Journal | View Issue

Open Access Article. Published on 24 October 2023. Downloaded on 12/6/2025 9:19:50 AM.
This article is licensed under a Creative Commons Attribution-NonCommercial 3.0 Unported Licence.

Check for updates

Cite this: *Green Chem.*, 2023, **25**, 9779

# Multimetallic Pd- and Ni-catalyzed C(sp$^2$)–P cross-coupling under aqueous micellar conditions†

Rafael Navrátil, * Kristýna Kellovská and Ondřej Baszczyński *

Organophosphorus compounds containing hydrolytically and metabolically stable C(sp$^3$)– and C(sp$^2$)–P bonds are widely used as reagents, ligands, pesticides, herbicides, flame retardants, surface modifiers, and antiviral and anticancer drugs. These applications rely on efficient C(sp$^3$)– and C(sp$^2$)–P bond-forming reactions. However, currently available C(sp$^2$)–P cross-coupling protocols require high catalyst loadings and temperatures, as well as environmentally unsustainable and harmful organic solvents (*e.g.*, *N*,*N*-dimethylformamide, DMF). Herein, we disclose a conceptually novel strategy for performing multimetallic Pd/Ni- and dual-ligand Pd-catalyzed C(sp$^2$)–P cross-coupling reactions in aqueous micelles under mild and environmentally friendly conditions. Micellar catalysis in water enables C(sp$^2$)–P cross-coupling while avoiding environmentally unsustainable organic solvents, thereby reducing organic waste generation. Such micellar C(sp$^2$)–P cross-coupling reactions tolerate various functional groups and provide access to structurally diverse (hetero)aryl (thio)phosphonates, phosphinates and phosphine oxides using inexpensive commercial materials and catalysts. Moreover, C(sp$^2$)–P cross-coupling reactions of medically relevant substrates and drugs under late-stage functionalization settings and multistep one-pot processes highlight the potential applications of this experimental paradigm.

Received 25th July 2023,
Accepted 23rd October 2023

DOI: 10.1039/d3gc02735j

rsc.li/greenchem

## Introduction

Phosphonates, phosphinates, phosphine oxides and related C–P bond-containing compounds are widely applied in organic[1] and pharmaceutical chemistry,[2,3] agrochemistry,[4] and materials science.[5,6] Introducing a C–P bond into organic compounds often improves their properties, increasing water solubility, decreasing lipophilicity, and enhancing pharmacokinetics.[7–9] Furthermore, C–P bonds are more metabolically stable than hydrolytically labile P–O bonds of natural phosphates.[8,10] Accordingly, the increased stability of C–P bonds has proved vital for numerous applications.

Isosterically replacing phosphates by more metabolically stable phosphonates has fostered the development of life-saving antiviral[11] and antibacterial[12] drugs and prodrugs[13] because they retain the bioactivity of the original phosphates.[10,14] Several bioactive phosphonates, phosphinates and phosphine oxides have also been applied in drug discovery and development,[2a,3,7,15–18] yielding fosdevirine, a non-nucleoside reverse transcriptase inhibitor (Fig. 1A),[19] and efonidipine, a calcium channel blocker,[20] in addition to eukaryotic initiation factor 4E (eIF4E) inhibitors.[21] Moreover, brigatinib, an anaplastic lymphoma kinase/epidermal growth factor receptor (EGFR) inhibitor[22] with an aryl dimethylphosphine oxide motif (Ar–P(O)Me$_2$), has been approved by the Food and Drug Administration (FDA) for cancer treatment. These applications of organophosphorus compounds rely on the development of efficient, practical, and scalable methods for the C(sp$^2$)–P bond construction.

C(sp$^2$)–P bonds are typically formed by cross-coupling (hetero)aryl and alkenyl (pseudo)halides and phenol derivatives with corresponding H–P compounds (*e.g.*, *H*-phosphonates, *H*-phosphinates, secondary phosphine oxides, diarylphosphines) under palladium,[23] nickel,[24] or copper[25] catalysis (also known as Hirao coupling, Fig. 1B).[26,27] However, current C(sp$^2$)–P cross-coupling methods are limited by (1) high catalyst loadings (often 10 mol %) and, in some cases, alternative procedures (slow addition of *H*-phosphonate)[28] or phosphorus precursors (*e.g.*, masked *H*-phosphonates)[29] required to overcome the inhibitory effects of phosphorus nucleophiles on metal catalysts given their strong coordination properties, (2) catalytic transfer hydrogenation, whereby (hetero)aryl halides are converted into (hetero) arenes due to the undesired reducing properties of H–P compounds,[30,31] (3) heating at high temperatures (often above 100 °C) to facilitate the C(sp$^2$)–P bond-forming reductive elimination step, rendering the reactions potentially incompatible with complex substrates bearing sensitive functional groups,

*Department of Organic Chemistry, Faculty of Science, Charles University, Hlavova 2030/8, 128 43 Prague 2, The Czech Republic.*
*E-mail: navratilr@natur.cuni.cz, baszczyo@natur.cuni.cz*

† Electronic supplementary information (ESI) available. See DOI: https://doi.org/10.1039/d3gc02735j

Open Access Article. Published on 24 October 2023. Downloaded on 12/6/2025 9:19:50 AM.
This article is licensed under a Creative Commons Attribution-NonCommercial 3.0 Unported Licence.

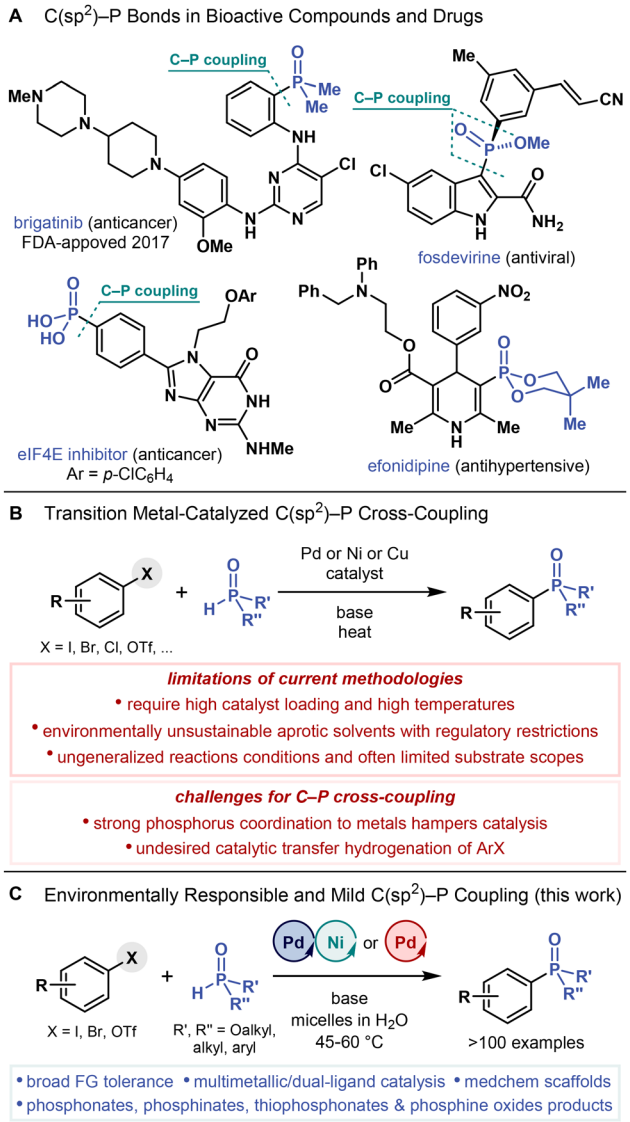


**Fig. 1** (A) Examples of bioactive organophosphorus compounds containing C(sp$^2$)–P bonds. (B) Conventional transition metal-catalyzed C(sp$^2$)–P cross-coupling reactions, their limitations, and obstacles to further developments. (C) C(sp$^2$)–P cross-coupling enabled by multimetallic Pd/Ni catalysis under mild micellar conditions in water (this work).

and (4) aprotic polar solvents, such as *N*,*N*-dimethylformamide (DMF),[24,32] which is classified as toxic and hazardous[33] and its use has been restricted by the European Commission.[34] Further exacerbating these problems, state-of-the-art C(sp$^2$)–P cross-coupling methods fail to meet increasing demands for environmentally responsible chemical processes with low energy costs and loadings of *precious* transition metal catalysts in environmentally benign solvents (*e.g.*, water[35]) under mild conditions (at room temperature or mild heating) while reducing organic waste generation.

A few studies on C(sp$^2$)–P cross-coupling in water have been reported (Fig. 2), but not without limitations. Under Pd catalysis, a single arylphosphonate has been synthesized from

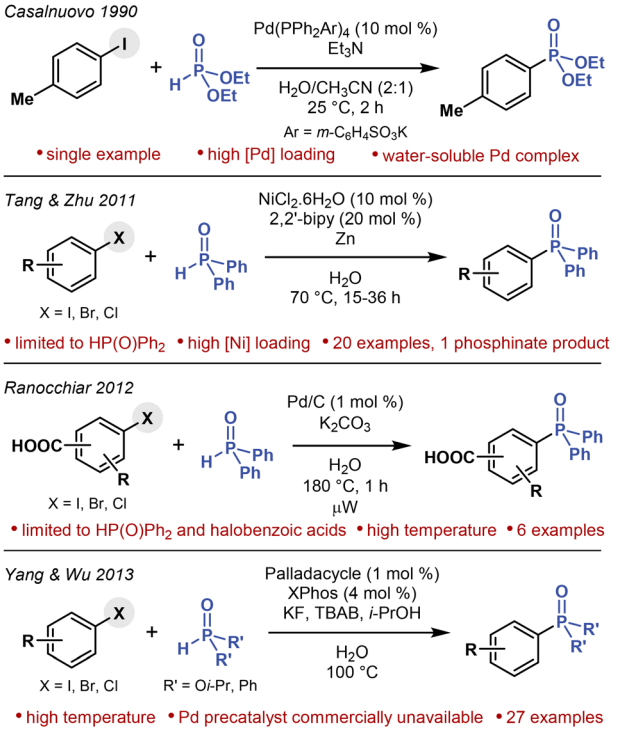


**Fig. 2** C(sp$^2$)–P cross-coupling reactions operating in water and their limitations.

4-iodotoluene and HP(O)(OEt)$_2$ at room temperature,[36] aryl phosphonates and phosphine oxides have been prepared from aryl halides and HP(O)(O*i*-Pr)$_2$ and HP(O)Ph$_2$, respectively, albeit at 100 °C,[37] and triaryl phosphine oxides have been synthesized from halobenzoic acids and HP(O)Ph$_2$ upon microwave irradiation at an even higher temperature (180 °C).[38] Under Ni catalysis, triaryl phosphine oxides have been synthesized from aryl halides and HP(O)Ph$_2$ at 70 °C.[39] Bar one, though, these methods require extensive heating. Moreover, they all show limited substrate scopes, predominantly providing triarylphosphine oxide products. Nevertheless, these precedents demonstrate that C(sp$^2$)–P cross-coupling reactions operating under aqueous conditions are feasible. In this context, we hypothesized that the current limitations of C(sp$^2$)–P cross-coupling methods could be overcome by performing C(sp$^2$)–P cross-coupling reactions under mild micellar conditions in water, a concept that is often referred to as micellar catalysis.

By micellar catalysis, organic compounds can be sustainably and efficiently synthesized in water, replacing traditional organic solvents.[40] In these processes, a small amount (a few wt %) of a surfactant is added into water to prepare micelles with lipophilic cores. These micelles help to solubilize otherwise water-insoluble organic compounds and serve as nanoreactors for their transformations. Several classes of organic reactions have already been adapted to micellar conditions in water, including transition metal-catalyzed cross-couplings,[41,42] amide-bond coupling,[43] and S$_N$Ar reactions,[44]

Open Access Article. Published on 24 October 2023. Downloaded on 12/6/2025 9:19:50 AM.
This article is licensed under a Creative Commons Attribution-NonCommercial 3.0 Unported Licence.

among others.[40] These reactions typically operate at room temperature (or under mild heating), require significantly lower catalyst loadings, produce much less waste, and show both faster reaction rates and better purity profiles than those run in conventional organic solvents. Yet, despite all these advantages, no C(sp$^2$)–P cross-coupling reaction has been performed under micellar conditions in water.

In this study, we describe the development of a mild, practical, general, and environmentally responsible C(sp$^2$)–P cross-coupling method, highlighting its applications in the synthesis of complex (hetero)aryl phosphonates, phosphinates and phosphine oxides (Fig. 1C). This method is enabled by a combination of (1) Pd- and Ni-based catalysts (*i.e.*, *multimetallic* catalysis), or (2) two Pd ligands (*i.e.*, *dual-ligand* catalysis). Moreover, our findings demonstrate the wide-ranging feasibility of a multimetallic catalytic process under micellar conditions in water.

**Table 2** Multimetallic Pd- and Ni-catalyzed C(sp$^2$)–P cross-coupling conditions under micellar catalysis conditions

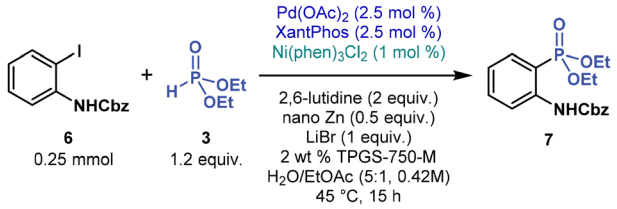


| Entry | Deviation from above | Yield[a] |
|---|---|---|
| 1 | None | 99% (94%)[b] |
| 2 | No [Pd], 2.5 mol% [Ni] | ND (87% RSM) |
| 3 | No [Ni], no Zn | 32% (63% RSM) |
| 4 | No Zn | ND (96% RSM) |
| 5 | Ni$^0$(COD)DQ/phen, no Zn | 14% (83% RSM) |

[a] Yields were determined by $^1$H NMR using $CH_2Br_2$ as an internal standard. [b] Isolated yield. RSM = recovered starting material. ND = not detected.

## Results and discussion

We developed a method for performing environmentally responsible micellar C(sp$^2$)–P cross-coupling reactions in water by screening suitable catalysts, ligands, bases and additives, as well as other reaction parameters (Tables 1–3). As a micellar catalyst, we used a well-established and commercially available "designer" surfactant TPGS-750-M (Table 1).[45] TPGS-750-M is a non-toxic, inexpensive, $\alpha$-tocopherol-based (vitamin E) amphiphile, which has been successfully used in numerous transition metal-catalyzed cross-coupling reactions in water.[40–42,45]

### Micellar C(sp$^2$)–P cross-coupling optimization

To optimize C(sp$^2$)–P cross-coupling under micellar conditions, we initially focused our efforts on Pd-catalyzed reactions. After extensively screening reaction conditions (Table 1, please refer to ESI† for more details), we determined that the

**Table 1** Initial optimization of micellar C(sp$^2$)–P cross-coupling reaction in water. All reactions were performed at 0.25 mmol scale

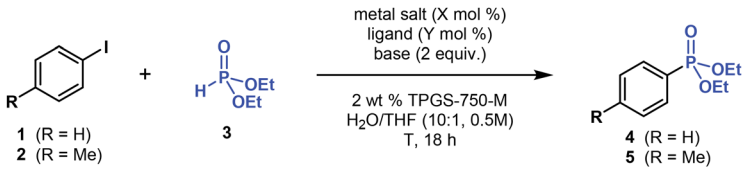


| Entry | R | ArI/3 ratio | Metal salt (X mol %) | Ligand (Y mol %) | Base | Deviation/additive | *T* | Yield[a] |
|---|---|---|---|---|---|---|---|---|
| 1 | H | 1.2/1 | $Pd(OAc)_2$ (5) | XantPhos (10) | $Et_3N$ | No THF | rt | 30% |
| 2 | H | 1.2/1 | $Pd(OAc)_2$ (5) | XantPhos (10) | $Et_3N$ | | 45 °C | 49% |
| 3 | H | 1.2/1 | $Pd(OAc)_2$ (5) | P(*t*-Bu)$_3$·HBF$_4$ (10) | $Et_3N$ | | 45 °C | 53% |
| 4 | H | 1.2/1 | $Pd(OAc)_2$ (5) | XantPhos (10) | 2,6-Lutidine | | 45 °C | 88% |
| 5 | H | 1.2/1 | $Pd(OAc)_2$ (1) | XantPhos (1) | 2,6-Lutidine | | 45 °C | 99% (91%)[b] |
| 6 | H | 1.2/1 | $Pd(OAc)_2$ (1) | XantPhos (1) | 2,6-Lutidine | 44 hours | rt | 88% |
| 7 | Me | 1.2/1 | $Pd(OAc)_2$ (1) | XantPhos (1) | 2,6-Lutidine | | 45 °C | 84%[c] (79%)[b] |
| 8 | Me | 1.2/1 | $Pd(OAc)_2$ (1) | XantPhos (1) | 2,6-Lutidine | LiCI (1 equiv.) | 45 °C | 94%[b] |
| 9 | Me | 1/2 | $Ni(XantPhos)Cl_2$ (5) | | $Et_3N$ | No THF, Zn (2 equiv.) | rt | ND |
| 10 | Me | 1/2 | $Ni(phen)Cl_2$ (2.5) | | 2,6-Lutidine[d] | LiCI (1 equiv.), nano Zn (0.5 equiv.) | 45 °C | 73%[c] |

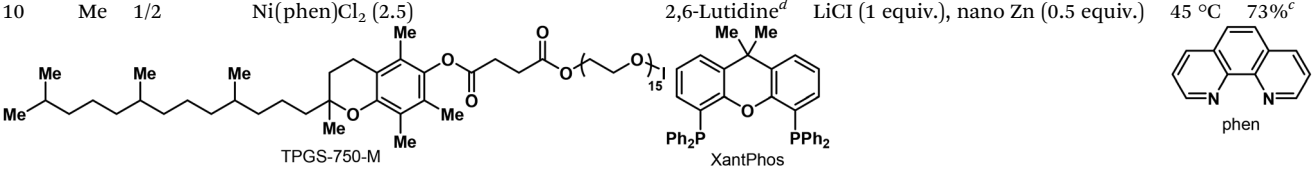


[a] Yield was determined by $^{31}$P NMR. [b] Isolated yield. [c] Yield was determined by $^1$H NMR using $CH_2Br_2$ as an internal standard. [d] 3 equiv. ND = not detected.

Open Access Article. Published on 24 October 2023. Downloaded on 12/6/2025 9:19:50 AM.
This article is licensed under a Creative Commons Attribution-NonCommercial 3.0 Unported Licence.

**Table 3** Dual-ligand C(sp$^2$)–P cross-coupling conditions under micellar catalysis conditions

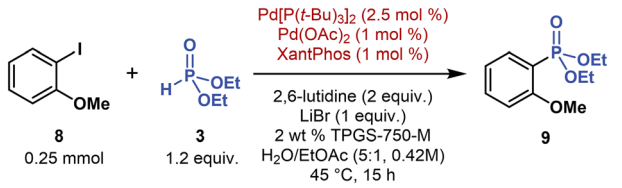


| Entry | Deviation from above | Yield[a] |
|---|---|---|
| 1 | None | Quant (99%)[b] |
| 2 | $Pd(OAc)_2/P(t\text{-}Bu)_3{\cdot}HBF_4$, no XantPhos | 24% (67% RSM) |
| 3 | No $Pd(OAc)_2$, no XantPhos | 47% (50% RSM) |
| 4 | No XantPhos | 13% (84% RSM) |
| 5 | No $Pd[P(t\text{-}Bu)_3]_2$ | ND (99% RSM) |
| 6 | $PCy_3{\cdot}HBF_4$ or $PMe(t\text{-}Bu)_2{\cdot}HBF_4$ | ND (99% RSM) |
| 7 | Multimetallic conditions (Table 2, entry 1) | 95% (full conv.) |

[a] Yields determined by $^1$H NMR using $CH_2Br_2$ internal standard. [b] Isolated yield. RSM = recovered starting material. ND = not detected. Please refer to additional optimization details in ESI.†

model coupling reaction of iodobenzene (**1**, 1.2 equivalent) with inexpensive diethyl *H*-phosphonate (**3**, 1 equivalent) provided the desired product, diethyl phenylphosphonate (**4**), in ~30% $^{31}$P NMR yield when using $Pd(OAc)_2$ (5 mol %), XantPhos (10 mol %), $Et_3N$ (2 equivalent), and 2 wt % TPGS-750-M in water (0.5 M), at laboratory temperature (~20 °C), over 18 hours (Table 1, entry 1). Adding an organic co-solvent (10 vol %), such as THF, into the reaction mixture and raising the temperature to 45 °C increased the yield of **4** (entry 2). After screening various mono- and bidentate phosphine ligands, including dppf, dppe, dppp, DPEphos, BINAP, dtbpf, Cy-XantPhos, $PCy_3$, $PMe(t\text{-}Bu)_2$, APhos and Buchwald-type (JohnPhos, DavePhos, XPhos, and SPhos) ligands, among others (see ESI†), we found that XantPhos and $P(t\text{-}Bu)_3$ (used as its bench-stable $HBF_4$ salt, entry 3) were the most effective ligands. Furthermore, decreasing catalyst loading from 5 to 1 mol % also improved the yield of **4** (entry 5).

The base used in this reaction strongly affected the yield. Switching from $Et_3N$ ($pK_{BH+}$ = 11.0 in $H_2O$) to a weaker but more lipophilic 2,6-lutidine base ($pK_{BH+}$ = 6.7 in $H_2O$) significantly improved the reaction yield (entry 4), affording **4** in 91% isolated yield. Stronger inorganic ($Cs_2CO_3$ and $K_3PO_4$) and organic (DBU, $Cy_2NMe$, and *t*-BuOK) bases proved ineffective (<5% yield by $^1$H NMR) and more lipophilic organic base $(n\text{-}Bu)_3N$ afforded **4** in 57% yield ($^1$H NMR). Therefore, micellar C(sp$^2$)–P cross-coupling requires using rather weak but more lipophilic bases, such as 2,6-lutidine, to achieve high yields.

The reaction with more electron-rich 4-iodotoluene (**2**) yielded phosphonate **5** in a lower yield of 79% (entry 7). Nevertheless, adding 1 equivalent of LiCl into the reaction mixture restored the high reaction yields, affording **5** in 94% yield (entry 8). Most likely, LiCl enhances the yield by decreasing the concentration of **2** dissolved in water (salting-out effect), thereby increasing the concentration and reaction rate of **2** in micellar compartments. Moreover, LiCl may generally enhance cross-coupling reactions.[46] As such, LiCl could have a twofold effect on micellar C(sp$^2$)–P coupling.

Subsequently, we tested alternative catalysts, namely Cu and Ni. Despite testing several Cu catalytic systems, no product was detected, in any case. Similarly, combining Ni(XantPhos)$Cl_2$ (5 mol %), $Et_3N$ (2 equivalent), and Zn powder (2 equivalent) provided no product (entry 9). But when combining $Ni(phen)_3Cl_2$ (2.5 mol %), 2,6-lutidine (3 equivalent), commercial nano Zn powder (0.5 equivalent), LiCl (1 equivalent) and THF co-solvent (10 vol %), we prepared **5** in 73% yield (see ESI† for more screening experiments). So at least for **2**, Ni catalysis did not match the efficiency of Pd catalysis. Based on these results, we identified Pd as an efficient catalytic system for micellar C(sp$^2$)–P coupling.

### Multimetallic catalysis

When applying the best performing reaction conditions (Table 1, entries 5 and 8) to other, electronically diverse substrates (*e.g.*, *N*-Boc-4-iodoaniline, 4-iodopyridine, 4-iodoanisole, and *N*-Cbz-2-iodoaniline), we initially observed little (<20%) to no product formation. At this point, we continued our extensive screening of ligands and reaction additives (see ESI†), eventually identifying efficient, general, *multimetallic* cross-coupling conditions. By combining Pd and Ni catalysts, C(sp$^2$)–P bonds were forged in aqueous micelles (Table 2). More specifically, cross-coupling of *N*-Cbz-2-iodoaniline (**6**, 1 equivalent) with **3** (1.2 equivalent) was catalyzed by $Pd(OAc)_2$ (2.5 mol %) with XantPhos (2.5 mol %) and $Ni(phen)_3Cl_2$ (1 mol %), in the presence of 2,6-lutidine (2 equivalent), commercial nano Zn powder (0.5 equivalent), and LiBr (1 equivalent, LiBr outperformed LiCl in most cross-couplings, see ESI†) in 2 wt % TPGS-750-M in water containing 16 vol % EtOAc co-solvent (the total concentration of **6** was 0.42 M). After stirring the reaction mixture at 45 °C, for 15 hours, phosphonate **7** was prepared in 94% yield (Table 2, entry 1). Therefore, under these reaction conditions, *multimetallic* catalysis promotes C(sp$^2$)–P cross-coupling.

Our control experiments confirmed that the palladium catalyst and zinc powder are essential; otherwise, no product is formed (Table 2, entries 2 and 4). The reaction without the nickel catalyst still provided **7**, but in a low yield (32% by $^1$H NMR), with most of **6** remaining unreacted (entry 3). Initially, we suspected that zinc only reduced Ni(II) to catalytically active Ni(0); however, the experiment with an air-stable Ni(0) precatalyst Ni(COD)DQ[47] without zinc provided **7** in only 14% yield ($^1$H NMR). These results indicate that zinc not only is a reductant but also facilitates transmetalation between Pd and Ni species, in line with previous multimetallic catalyzed C(sp$^2$)–C(sp$^2$) cross-coupling reactions.[48]

By adding a small amount (5–20 vol %) of an organic co-solvent into a reaction run in micelles, we were able to overcome the limited solubility of some starting compounds (*vide infra*) and to maintain a stable emulsion throughout the reaction, thereby increasing reaction rates and yields.[49] Using EtOAc as a co-solvent ($H_2O$ : EtOAc in 5 : 1 v/v ratio) proved more advantageous than THF (or any other solvent tested in

Open Access Article. Published on 24 October 2023. Downloaded on 12/6/2025 9:19:50 AM.
This article is licensed under a Creative Commons Attribution-NonCommercial 3.0 Unported Licence.

this study, such as toluene, 1,4-dioxane, and acetone, among others), mainly because EtOAc (i) slightly increased the reaction yields, possibly due to the higher solubilizing power of organic compounds, and/or micelle expansion, and is (ii) ranked as a green solvent[33] (iii) also used during extraction work-up.

Our micellar C(sp$^2$)–P coupling method is both simple and practical, and its progress can be monitored by standard TLC or LC-MS analysis. When the reaction is finished, the product is extracted by adding a small volume of EtOAc (3 × ∼1 mL for a 0.25 mmol-scale reaction) directly into the reaction vial/flask, subsequently evaporating volatiles. If desired, an excess of **3** and 2,6-lutidine can also be evaporated under high-vacuum.[50] The crude product is then purified by chromatography. In some cases (*vide infra*), the product can be conveniently isolated in sufficient purity simply by filtering the reaction mixture or by directly injecting the reaction mixture onto a reverse-phase column chromatography column and performing the chromatography separation. The latter is particularly advantageous for isolating highly water-soluble phosphine oxide products (Fig. 5).

Some *multimetallic* Pd/Ni C(sp$^2$)–P cross-couplings were problematic, particularly those with strongly coordinating phosphorus nucleophiles (*e.g.*, secondary phosphine oxides) or with electron-rich aryl iodides and bromides. Difficulties with the latter resulted from stronger C–I and C–Br binding, which complicated oxidative addition into these bonds. Both issues proved relevant when establishing the substrate scope of aryl halides and phosphorus nucleophiles (Fig. 3–5).

### *Dual-ligand* conditions

In our initial screening under *single-metal* Pd catalysis (Table 1, entry 3), we identified the bulky, electron-rich P(*t*-Bu)$_3$ ligand as the second most efficient ligand. This ligand facilitated both oxidative addition to stronger C–halogen bonds and cross-coupling with strongly coordinating phosphorus nucleophiles, such as secondary phosphine oxides (Fig. 5, see ESI† for further experiments). To understand the effect of the P(*t*-Bu)$_3$ ligand on Pd-catalyzed C(sp$^2$)–P couplings under micellar conditions, we performed several reactions of electron-rich 2-iodoanisole (**8**, 1 equivalent) with **3** (2 equivalent) and Pd(OAc)$_2$ (5 mol %) and P(*t*-Bu)$_3$·HBF$_4$ (10 mol %) (Table 3, entry 2). For a direct comparison with *multimetallic* conditions, we used the same base (2,6-lutidine), additive (LiBr), and co-solvent (EtOAc).

The reaction between **8** and **3** using the P(*t*-Bu)$_3$ ligand afforded **9** in 24% yield ($^1$H NMR with $CH_2Br_2$ as an internal standard), whereas the reactions using other bulky, electron-rich trialkyl phosphine ligands (PCy$_3$, PMe(*t*-Bu)$_2$) provided no detectable product (Table 3, entry 6). Coupling **8** with **3** using a commercially available Pd[P(*t*-Bu)$_3$]$_2$ catalyst (5 mol %) nearly doubled the yield of **9**, reaching 47% (entry 3). But when we combined Pd[P(*t*-Bu)$_3$]$_2$ (2.5 mol %) with Pd(OAc)$_2$ (1 mol %) and XantPhos (1 mol %), **9** was formed almost quantitatively. Thus, the yield of challenging C(sp$^2$)–P cross-coupling reactions may be optimized under *dual-ligand* conditions.

Under *dual-ligand* conditions, further control experiments showed that both P(*t*-Bu)$_3$ and XantPhos ligands are essential. Without XantPhos, the yield of **9** decreased from a virtually quantitative yield to 13% (Table 3, entry 4). Without Pd[P(*t*-Bu)$_3$]$_2$, **9** was not detected (entry 5). Similar dual-ligand synergic effects have been previously described in Pd-catalyzed reactions, for example, in arene C–H functionalization,[51] decarboxylative desaturation,[52] and ketone α-alkylation.[53]

Based on our experimental data on *dual-ligand* C(sp$^2$)–P coupling, oxidative addition to the C–halogen bond may be promoted by a bulky, electron-rich P(*t*-Bu)$_3$ ligand. This ligand effectively competes for coordination to Pd(0) centers with nucleophilic **3**, presumably in its trivalent phosphite form (P(OH)(OEt)$_2$). In turn, reductive elimination, forging the C(sp$^2$)–P bond, may be facilitated by the high-bite-angle (111°) bidentate XantPhos ligand,[54,55] which preferentially coordinates to Pd(II) intermediates (see ESI† for plausible mechanism).[56] The C(sp$^2$)–P cross-coupling mechanism is likely more complex because acetates, derived from either Pd(OAc)$_2$ or added KOAc (tested during screening experiments), also facilitated C(sp$^2$)–P coupling; this positive acetate effect on C(sp$^2$)–P cross-coupling has been previously reported, albeit in reactions performed in traditional organic solvents.[23c] Therefore, *multimetallic* and *dual-ligand* conditions provide complementary access to C(sp$^2$)–P cross-coupling products (*vide infra*).

### Substrate scope of aryl halides

We applied both optimized conditions (*multimetallic* Conditions A: Pd(OAc)$_2$/XantPhos/Ni(phen)$_3$Cl$_2$/nano Zn; *dual-ligand* Conditions B: Pd[P(*t*-Bu)$_3$]$_2$/Pd(OAc)$_2$/XantPhos) in cross-coupling reactions of several aryl iodides and bromides with *H*-phosphonate **3** (Fig. 3). The methods proved effective in a wide range of electron-rich and electron-poor substrates, affording phosphonate products (**5**, **7**, **9–49**) in high yields, including those with hydroxyl (**11**), amino (**13**), benzamide (**18**), carboxylic acid (**19**), ketone (**26**), and pinacol boronate (**25**, **44**) groups. These results demonstrate the excellent functional group-tolerance of micellar C(sp$^2$)–P cross-coupling.

Highly crystalline substrates, such as 4-iodonitrobenzene and aryl iodide precursors of phosphonates **43** and **44**, required a higher dilution (0.21 M instead of 0.42 M) because of their poor solubility. Other substrates also demanded introducing some modifications, namely using Pd[P(*t*-Bu)$_3$]$_2$ catalyst (5 mol %) with KOAc additive (0.5 equivalent) and running the reaction at a higher temperature (55 °C), to prevent potential inhibitory effects of nucleophilic (NH$_2$ and NMe$_2$) functional groups on cross-coupling. Under these slightly modified conditions, we prepared phosphonates **13** and **14** in 59 and 70% yields, respectively.

Aryl iodides containing Br and OTf groups, which are typically also reactive in cross-coupling reactions, provided the corresponding phosphonates **23** and **24** in 45 and 63% yields, along-side bis-phosphonate **47**. The side-product **47** was formed even when we performed cross-coupling with only 1.2 equivalents of **3** and at a decreased reaction temperature

Open Access Article. Published on 24 October 2023. Downloaded on 12/6/2025 9:19:50 AM.
This article is licensed under a Creative Commons Attribution-NonCommercial 3.0 Unported Licence.

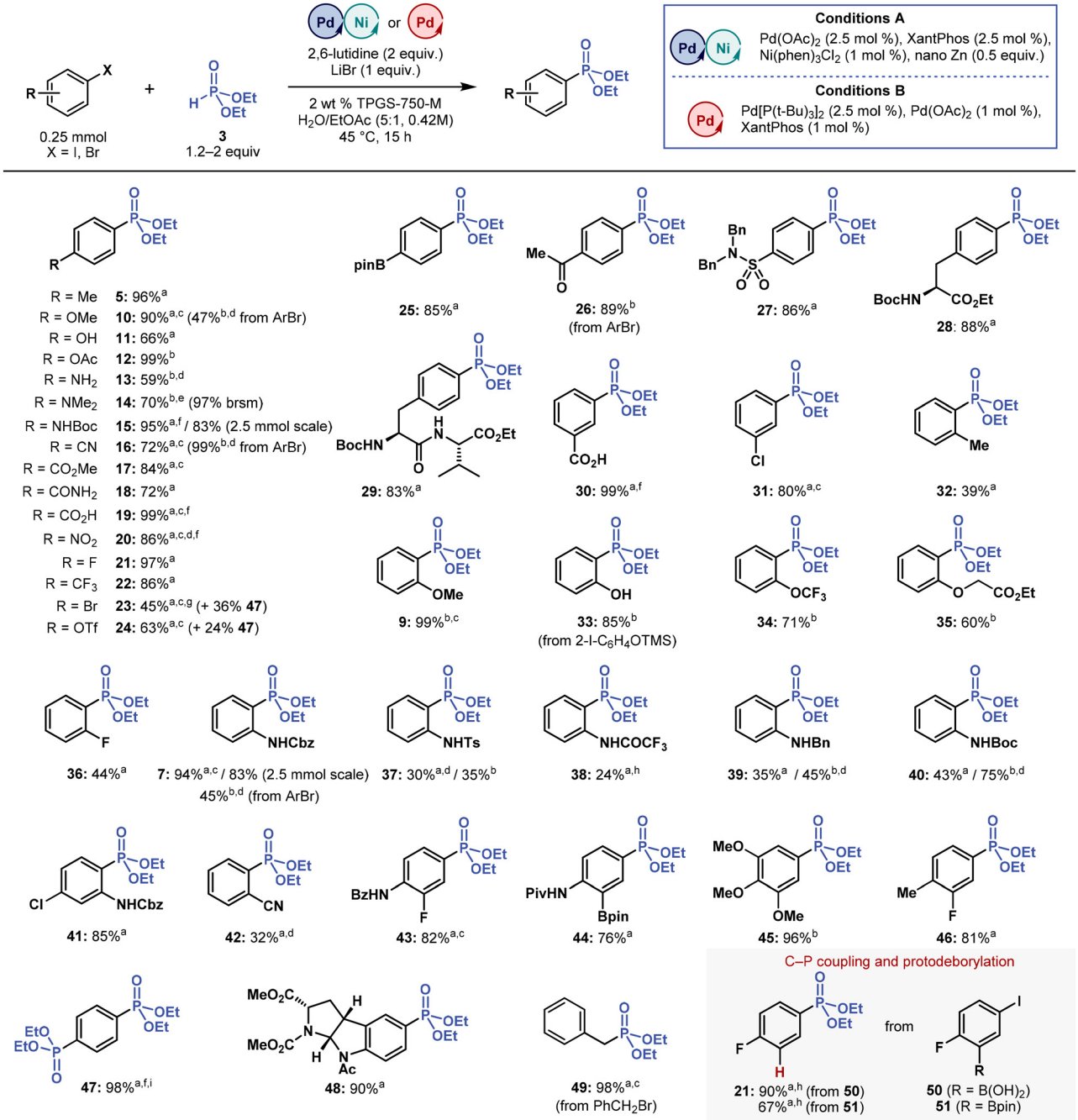


**Fig. 3** Substrate scope of multimetallic-catalysed micellar C(sp$^2$)–P cross-coupling towards aryl halides. Isolated yields are reported, unless noted otherwise. [a]Conditions A. [b]Conditions B. [c]1.2 equivalent of **3**. [d]Performed at 55 °C. [e]Performed at 60 °C. [f]3 equivalents of 2,6-lutidine. [g]Performed at 35 °C. [h]Determined by $^1$H NMR with internal standard. [i]3 equivalents of **3**. brsm = based on recovered starting material. Please refer to ESI† for more details.

(35 °C). This outcome demonstrates that the reactivity of **23** and **24** is, at least, on a par with that of corresponding starting aryl iodides. If desired, **47** can be synthesized directly by coupling 1,4-diiodobenzene to **3** (3 equivalent) in an almost quantitative yield.

Notwithstanding the results described above, micellar C(sp$^2$)–P coupling proved highly sensitive to *ortho* substitution on an aromatic ring in most aryl halides. Broadly speaking, Conditions B provided higher yields of *ortho*-substituted phosphonates than Conditions A despite using the bulky P(*t*-Bu)$_3$ ligand. Under Conditions A, only phosphonates **9** (*o*-OMe, 99% yield using Conditions B), **7** (*o*-NHCbz, 94% yield using Conditions A from ArI, 45% using Conditions B from ArBr), and **41** (85%, Conditions A) were formed in high yields.

Open Access Article. Published on 24 October 2023. Downloaded on 12/6/2025 9:19:50 AM.
This article is licensed under a Creative Commons Attribution-NonCommercial 3.0 Unported Licence.

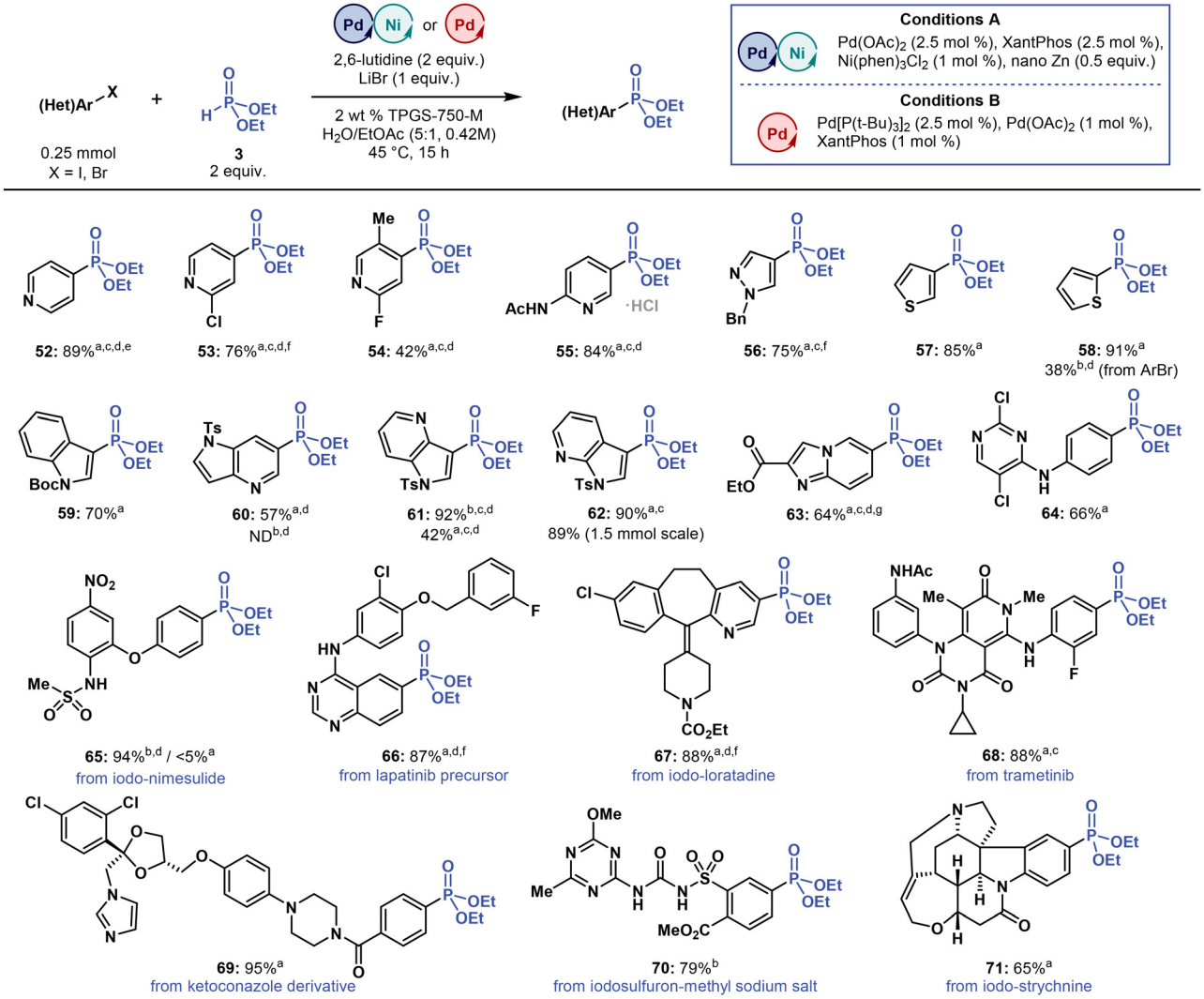


**Fig. 4** Substrate scope of multimetallic-catalysed micellar C(sp$^2$)–P cross-coupling towards heteroaryl iodides and medically relevant compounds. Isolated yields are reported. [a]Conditions A. [b]Conditions B. [c]3 equivalent of 2,6-lutidine. [d]Performed at 55 °C. [e]5 mol% of Ni(phen)$_3$Cl$_2$. [f]2.5 mol% of Ni(phen)$_3$Cl$_2$. [g]4 equivalents of **3**. ND = not detected. Please refer to ESI† for more details.

Phosphonates with other *ortho* substituents (Me, $OCF_3$, $OCH_2CO_2Et$, F and CN) were formed in low-to-good yields (32–61%), whereas some *ortho* substituents (OH, $CO_2H$, $CO_2Me$, $CONH_2$ and $NO_2$) were incompatible with the reaction conditions, generating products in trace amounts or in less than 20% yield ($^1$H NMR). In addition, *o*-OH phosphonate **33** was accessed in 85% yield by coupling (2-iodophenoxy)trimethylsilane with **3**. This finding indicates that C(sp$^2$)–P cross-coupling shows faster kinetics than silyl ether hydrolysis under aqueous micellar conditions.

When assessing in more detail the *ortho* substituent effect on 2-iodoaniline derivatives, we found that **7** (*o*-NHCbz) was produced in 94% yield, whereas **37** (*o*-NHTs), **38** (*o*-NHCOCF$_3$), and **39** (*o*-NHBn) were formed in low-to-moderate yields ranging from 24 to 45%, irrespective of the conditions (A and B). Under these cross-coupling Conditions A and B, **40** (*o*-NHBoc) was formed in much higher yields of 43 and 75%, respectively. But replacing hydrogen with methyl in the *o*-NHBoc group (*o*-NMeBoc) completely inhibited this reaction, possibly due to increased steric hindrance, confirming that cross-coupling reactions are affected by steric effects of *ortho* substituents. However, these steric effects alone do not explain the differences in the yields of phosphonates **7**, **37–40**. Differences in the acidity of the adjacent N–H group may also affect the efficiency of micellar C(sp$^2$)–P coupling.

In coupling reactions with boronic acid **50** and pinacol boronate **51**, the expected phosphonate products were not formed; instead, phosphonate **21** was formed in high yields, in both reactions, through a sequential C(sp$^2$)–P coupling and an undesired base-promoted protodeborylation. Protodeborylation is a known side-reaction in the cross-coupling chemistry of base-sensitive fluorine-containing boronic acids and pinacol esters.[57] To avoid this undesired reaction, we performed an additional experiment with only 1.2 equiva-

Open Access Article. Published on 24 October 2023. Downloaded on 12/6/2025 9:19:50 AM.
This article is licensed under a Creative Commons Attribution-NonCommercial 3.0 Unported Licence.

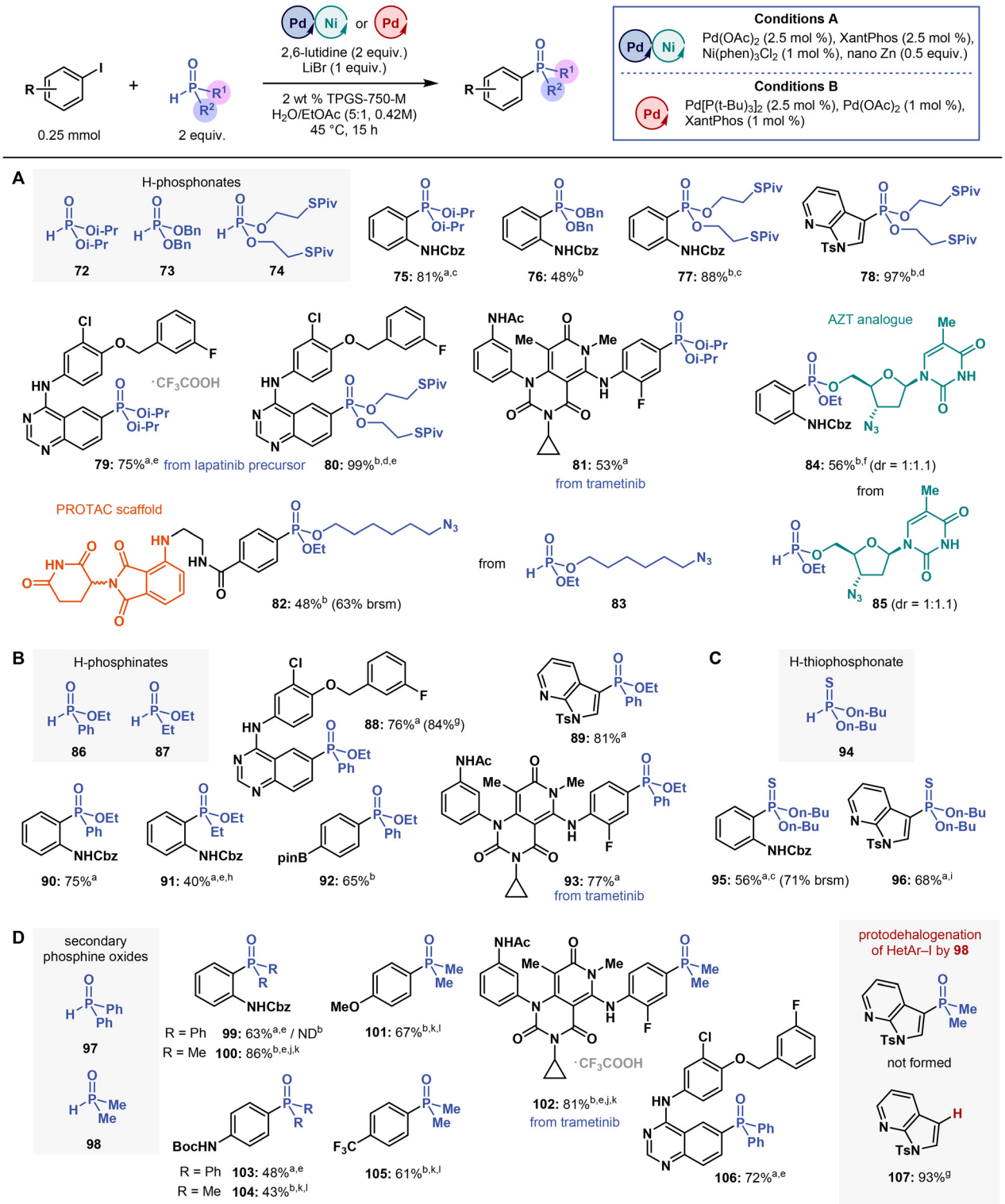


**Fig. 5** Substrate scope of H–P compounds in the multimetallic-catalysed micellar C(sp$^2$)–P cross-coupling. Isolated yields are reported. [a]Conditions A. [b]Conditions B. [c]1.2 equivalent of H–P compound. [d]1.5 equivalent of **74**. [e]Performed at 55 °C. [f]1 equivalent of **85**, 1.2 equivalent of **6**. [g,l]H NMR yield using $CH_2Br_2$ as an internal standard. [h]2.5 mol% of $Ni(phen)_3Cl_2$, 3 equivalents of 2,6-lutidine. [i]2.1 equivalents of **94**. [j]3 equivalents of **98**. [k]3 equivalents of *N*-methylmorpholine instead of 2,6-lutidine. [l]Performed at 60 °C. brsm = based on recovered starting material. ND = not detected. Please refer to ESI† for more details.

Open Access Article. Published on 24 October 2023. Downloaded on 12/6/2025 9:19:50 AM.
This article is licensed under a Creative Commons Attribution-NonCommercial 3.0 Unported Licence.

lents of **3** and 1.2 equivalents of 2,6-lutidine, but **21** was still the main reaction product.

### Substrate scope of heteroaryl halides and/or medicinally relevant compounds

Applying the best reaction conditions thus far to C(sp$^2$)–P coupling of heteroaryl iodides and bromides with **3** (Fig. 4) required decreasing the concentration of most starting compounds to 0.21 M to improve their solubilization and increasing the reaction temperature to 55 °C to reach higher conversion rates. As a co-solvent, EtOAc was also essential, outperforming all other organic co-solvents (THF, acetone and toluene) tested in this study. Cross-coupling reactions with 4- and 3-iodopyridines, *N*-benzyl-3-iodopyrazole, 2- and 3-iodothiophenes, and *N*-Boc-3-iodoindole provided the corresponding phosphonates (**52–59**) in yields ranging from 70 to 91%. The exception was phosphonate **54**, which was formed in only 42% yield, most likely due to steric hindrance.

Reactions of medicinally relevant 4- and 7-azaindoles with **3** provided phosphonates **60–62** in yields ranging from 57 to 92%. In particular, phosphonate **61** was formed in 92 and 42% yields when we applied Conditions B (*dual-ligand*) and A (*multimetallic*), respectively, thus showcasing the strong correlation between yield and reaction conditions. The medicinally relevant, nitrogen-rich phosphonates **63** and **64** were obtained in 64 and 66% yields, respectively, and even the starting aryl iodide for **64** was also prepared under micellar conditions in water ($S_NAr$ reaction). Therefore, micellar C(sp$^2$)–P cross-coupling provides us with access to heterocyclic phosphonates potentially relevant to the discovery and development of bioactive compounds.

When applied to drug-like scaffolds and drugs with various functional groups (Fig. 4), these micellar C(sp$^2$)–P coupling conditions were also effective. Reactions with iodinated drugs and bioactive compounds, specifically iodo-nimesulide, iodo-loratadine, iodo-strychnine, provided the respective phosphonates **65**, **67** and **71** in yields ranging from 65 to 94%. Coupling with the key lapatinib (anticancer drug) synthetic precursor[58] and with bioactive iodine-containing compounds, such as trametinib (anticancer drug) and iodosulfuron-methyl sodium salt (sulfonylurea herbicide), also afforded phosphonates **66**, **68**, and **70** in high yield of 87, 88, and 79%, respectively. Among these drug-like scaffolds and drugs, the highest yield (95%) was achieved when preparing phosphonate **69** from an antifungal ketoconazole derivative. These findings demonstrate that micellar C(sp$^2$)–P cross-coupling reactions can be tolerated by a wide range of functional groups of drug scaffolds, providing opportunities for late-stage modifications.

### Substrate scope of H–P(O) compounds

After establishing the substrate scope for (hetero)aryl halide couplings with diethyl *H*-phosphonate (**3**), we examined cross-coupling reactions with other phosphorus partners containing H–P bonds, such as other *H*-(thio)phosphonates, *H*-phosphinates, and secondary phosphine oxides (SPOs) (Fig. 5). In solution, these compounds feature prototropic tautomerism between their electrophilic tetravalent P(═O)H and nucleophilic trivalent P–OH forms.[59] The latter carry a lone electron pair, which is responsible for phosphorus coordination to transition metals.[60] Unsurprisingly, the electron-withdrawing and -donating substituents on the phosphorus centre strongly affected the tautomerization equilibria and their rates, as previously shown by an experimental and theoretical study with a series of $R^1R^2P(O)H$ compounds, wherein tautomerization rates considerably decreased in the following order: $Ph_2P(O)H$ > PhP(O)(OAlk)H > AlkP(O)(OAlk)H > $(AlkO)_2P(O)H$ (Alk = alkyl).[59] As such, substituents attached to phosphorus inherently affect all reactions involving equilibria between P(═O)H and P–OH tautomers in solution under both basic and acidic conditions,[61] including transition metal-catalyzed reactions. This effect explains why developing a general set of conditions for cross-coupling structurally diverse phosphorus compounds can be a challenging task.

At first, we studied the reactivity of different *H*-phosphonates, more specifically di-iso-propyl *H*-phosphonate (**72**), dibenzyl *H*-phosphonate (**73**), and bis-(*S*-pivaloyl-2-thioethyl) *H*-phosphonate (**74**). All of them efficiently coupled with aryl halides under optimized reaction conditions, except for **73**, which is hydrolytically labile and thus afforded product in low yield (Fig. 5A). Cross-coupling reactions with **74** provided direct access to phosphonates **77**, **78** and **80** bearing a *S*-acylthioethyl (SATE, specifically *S*-pivaloyl-2-thioethyl group)[62] prodrug moiety in high yields, ranging from 88 to 99% (Fig. 5A). Coupling reactions of the lapatinib precursor and trametinib with **72** afforded phosphonates **79** and **81**, in 75 and 53% yields, respectively. Other, commercially available dimethyl and di-*n*-butyl *H*-phosphonates showed the same efficiency as **3** (data not shown; both phosphonates were used in preliminary screening experiments; see ESI†), but the sterically hindered di-*tert*-butyl *H*-phosphonate failed to afford the target products under our reaction conditions.

To further demonstrate the functional group tolerance of the micellar C(sp$^2$)–P coupling method and its application potential in medicinal chemistry, we cross-coupled a pomalidomide derivative, frequently used in emerging proteolysis targeting chimera (PROTAC) technology,[63] with a *H*-phosphonate **83** containing a "clickable" terminal azide (Fig. 5A). In this coupling, we prepared phosphonate **82** in 48% yield (63% brsm) using Conditions B (without any further optimization). Accordingly, **82** may be applied in PROTAC technology upon a copper-catalysed click reaction with a suitable alkyne linker connected to an inhibitor of interest. The third phosphorus substituent, the ethoxy group, may also be exchanged for an additional functionality, thereby further expanding PROTAC applications.

We also synthesized *H*-phosphonate **85**, an analogue of the antiviral drug azidothymidine (AZT), and subjected **85** to C(sp$^2$)–P cross-coupling with **6** (Fig. 5A). In this reaction, 1 equivalent of **85** was mixed with 1.2 equivalents of iodide **6** under Conditions B, affording the desired AZT-containing phosphonate **84** in 56% yield and in a 1 : 1.1 diastereomeric ratio ($^{31}$P NMR). These reactions demonstrate that C(sp$^2$)–P

Open Access Article. Published on 24 October 2023. Downloaded on 12/6/2025 9:19:50 AM.
This article is licensed under a Creative Commons Attribution-NonCommercial 3.0 Unported Licence.

coupling in water may be used to synthesize potentially bioactive nucleoside analogues in medicinal chemistry.[64]

Despite their structural differences from *H*-phosphonates, two *H*-phosphinates, namely ethyl phenyl- (**86**) and ethyl ethyl-*H*-phosphinate (**87**), the latter being relevant to the synthesis of CDK9/CycT1 inhibitors,[18] also reacted under micellar cross-coupling conditions. Cross-coupling reactions with **86** provided the corresponding phosphinates **88–90**, **92** and **93** in yields ranging from 65 to 78% (Fig. 5B), including a trametinib derivative. But the reactions with *H*-phosphinate **87** were challenging, and we prepared only phosphinate **91** in 40% yield notwithstanding our efforts to optimize the reaction conditions specifically for **87**. Under Conditions B or in reactions with other ligands or bases, **91** was formed in less than 20% yield, as shown by $^1$H NMR analysis (see ESI†). These results are in line with studies on cross-coupling reactions with **87**, which also reported low yields, even under more forcing conditions (refluxing toluene).[23fg] These stark differences in cross-coupling reactivity between **86** and **87** may be attributed to their different P(═O)H/P–OH tautomerization rates[59] and to the stronger electron-donating abilities of the ethyl group in **87**. In line with these explanations, the phosphorus in **87** shows increased electron density, which strengthens its binding to metal centres, possibly inhibiting the catalytic activity of these metal centres.

Although only a few studies on cross-coupling reactions with *H*-thiophosphonates (containing a P═S bond) have been published thus far,[65] we assessed whether *H*-thiophosphonates, such as **94**, prepared by treating di-*n*-butyl *H*-phosphonate with Lawesson's reagent, could also be coupled with aryl iodides under micellar C(sp$^2$)–P coupling conditions. Upon coupling with aryl iodides, the desired *H*-thiophosphonates were formed in poor yields (<30%), but we eventually found that the excess of **94** (and possibly of thiophosphonate products as well) inhibited the reaction. When we performed the coupling reaction by adding 0.7 equivalents of **94** in three portions (2.1 equivalents in total), the thiophosphonates **95** and **96** were formed in 56% (71% brsm) and 68% yields, respectively (Fig. 5C). Under our conditions, cross-couplings with ethyl phenyl-*H*-thiophosphinate (prepared in a reaction of **86** with Lawesson's reagent) failed presumably because this phosphinate has strong coordination properties, which inhibit metal catalysis, similar to those of sulfur compounds. To the best of our knowledge, no metal-catalysed coupling reaction with alkyl aryl-*H*-thiophosphinate has been reported to date.

Lastly, we performed cross-coupling reactions with secondary phosphine oxides (SPOs) **97** and **98** (Fig. 5D). SPOs are used not only as coupling partners but also as versatile ligands for their strong binding to metal centres.[66] For this reason, cross-coupling reactions with SPOs often require high catalyst loadings (10–20 mol%) and temperatures ranging between 90 to 120 °C,[67] so we expected that micellar cross-coupling reactions with SPOs could be challenging. Yet, under Conditions A (Conditions B were ineffective), C(sp$^2$)–P coupling reactions with diphenyl phosphine oxide (**97**) afforded the corresponding triaryl phosphine oxides **99**, **103** and **106** in good yields (43–72%) (Fig. 5D). In contrast, under modified Conditions B (Conditions A were ineffective), the reactions with dimethyl phosphine oxide (**98**) afforded highly-polar phosphine oxides **100–102**, **104** and **105** in yields ranging from 43 to 81%.

The cross-coupling reactions with **98** required using a stronger base than 2,6-lutidine (*N*-methylmorpholine; $pK_{BH^+}$ = 7.4 in $H_2O$) and, most often, increasing the reaction temperature to 60 °C to enhance conversion. Overall, these reactions were challenging. For example, no phosphine oxide was formed from the 3-iodo-7-azaindole derivative; instead, the starting compound was cleanly converted into the corresponding protodehalogenation product **107** (93% by $^1$H NMR with $CH_2Br_2$ as an internal standard) (Fig. 5D). Substituting Ts for Boc as the protecting group made no difference in the reaction outcome either. So, in some reactions, **98** acts as a hydrogen donor in a Pd-catalyzed transfer hydrogenation process, as do hypophosphites.[30,31] Furthermore, our results corroborate the findings of a previous report on catalytic transfer hydrogenations of alkyl and aryl halides by sodium hypophosphite under micellar conditions in water (Tween 20 surfactant).[68] Similarity to *H*-phosphinates, the reactivity differences between **97** and **98** may stem from their distinct P(═O)H/P–OH tautomerization rates,[59] possibly explaining the effect of base, and from stronger binding of **98** to Pd catalyst. Therefore, micellar cross-coupling reactions with **98** require using a more strongly coordinating and bulky P(*t*-Bu)$_3$ ligand and more forcing conditions (heating to 60 °C).

### Scale-up experiments

We also performed reactions at 1.5–2.5 mmol scales to understand how micellar C(sp$^2$)–P cross-couplings proceed at larger reaction scales. The yields of phosphonates **7** (83% at 2.5 mmol *vs.* 94% at 0.25 mmol), **62** (89% at 1.5 mmol *vs.* 90% at 0.25 mmol) and **15** (83% at 2.5 mmol *vs.* 95% at 0.25 mmol) were slightly lower in these reactions than in those at the original reaction scale (Fig. 3 and 4). Moreover, the scale-up synthesis of **7** was performed with half the original catalyst loading (1.25 mol% Pd and 0.50 mol% Ni), thus demonstrating that catalyst loadings can be reduced in cross-coupling reactions with strongly coordinating phosphorus nucleophiles such as **3**.

### Tandem processes involving C(sp$^2$)–P cross-coupling

Dialkyl *H*-phosphonates are typically prepared by mixing alcohols with toxic, moisture- and air-sensitive $PCl_3$.[69] As such, *H*-phosphonate syntheses are impractical and hazardous and often lead to intractable mixtures of products.[70] Dialkyl *H*-phosphonates can also be prepared by transesterification of diphenyl *H*-phosphonate (**108**).[71] In this process, **108** is mixed with an alcohol under basic (pyridine) and neat conditions, thereby completely avoiding corrosive $PCl_3$. For this reason, we assessed whether commercial diphenyl *H*-phosphonate (**108**) can be used as an inexpensive ($0.50 per gram at Sigma-Aldrich) source of dialkyl *H*-phosphonates formed *in situ* and

Open Access Article. Published on 24 October 2023. Downloaded on 12/6/2025 9:19:50 AM.
This article is licensed under a Creative Commons Attribution-NonCommercial 3.0 Unported Licence.

then directly, without isolation, converted into arylphosphonates in micellar C(sp$^2$)–P cross-coupling, in a one-pot process.

As a proof-of-concept, we treated neat, technical grade **108** (<90% purity, 2 equivalents) with EtOH (4 equivalents) and 2,6-lutidine (4 equivalents) at room temperature for 3 hours (**3** formed *in situ*), subsequently adding **6** (1 equivalent), Pd/Ni catalyst, LiBr, 2,6-lutidine, 2 wt % TPGS-750-M in water (0.5 mL), and EtOAc (0.1 mL) into the reaction mixture (Fig. 6A). After stirring for 15 hours, at 45 °C, phosphonate **7** was formed in 80% yield from **108** and EtOH (*vs.* 94% from **3** with **6**). This experiment demonstrates that dialkyl *H*-phosphonates can be prepared from inexpensive and bench-

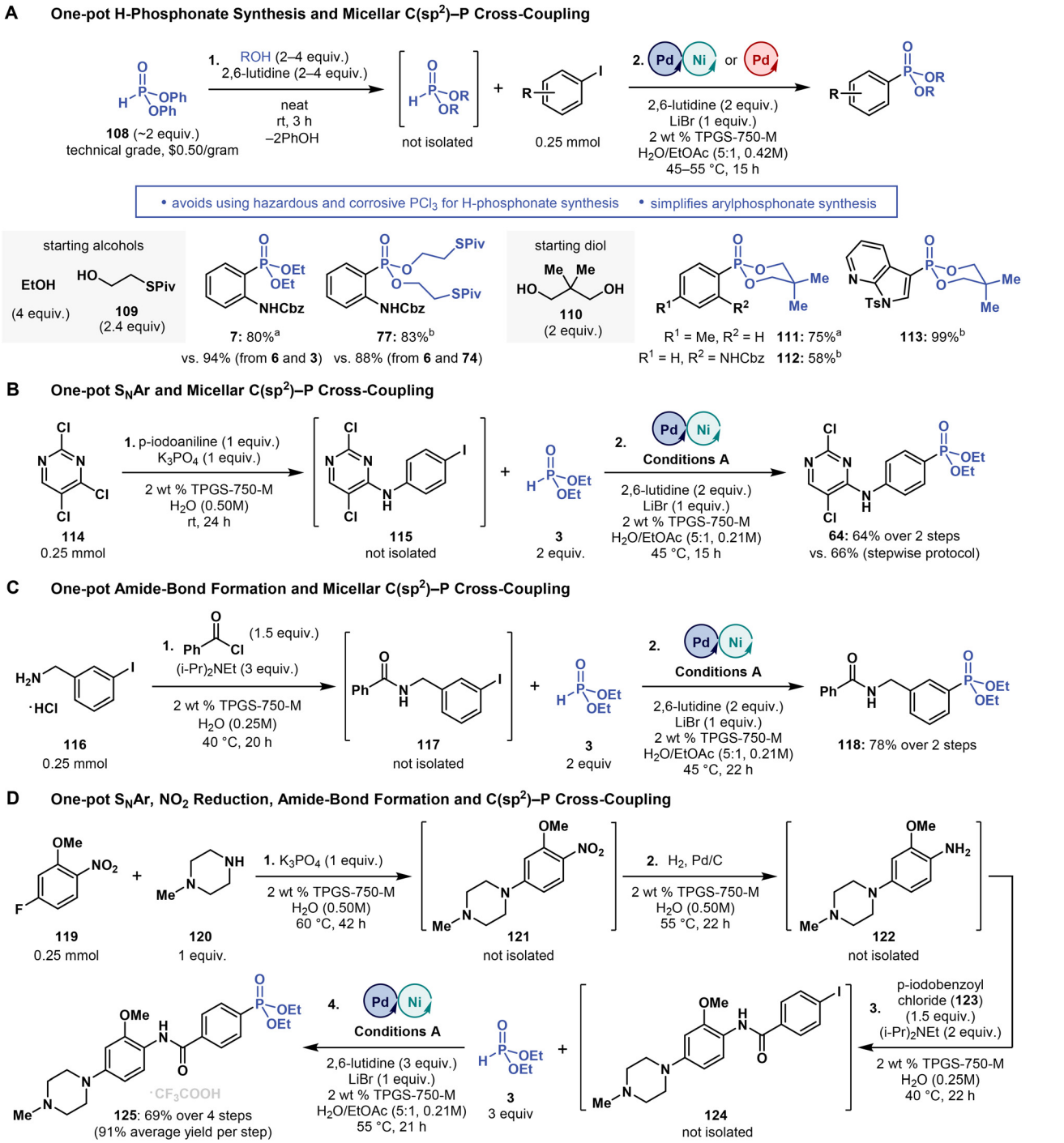


**Fig. 6** Tandem processes involving micellar C(sp$^2$)–P cross-coupling. (A) Using diphenyl *H*-phosphonate (**108**) enables a two-step, one-pot aryl phosphonate synthesis involving the *in situ* formation of dialkyl *H*-phosphonates from alcohols. (C) Multistep one-pot processes involving C(sp$^2$)–P cross-coupling. [a]Conditions A. [b]Conditions B (see Fig. 3–5). Please refer to ESI† for more details.

Open Access Article. Published on 24 October 2023. Downloaded on 12/6/2025 9:19:50 AM.
This article is licensed under a Creative Commons Attribution-NonCommercial 3.0 Unported Licence.

stable **108** and then directly used in micellar C(sp$^2$)–P cross-coupling reactions. Moreover, the cross-coupling step is robust enough to tolerate phenol by-product, with only negligible decreases in reaction yields.

We also prepared **77** in 83% yield (*vs.* 88% from **6** and **74**) from **74**, which was formed *in situ* from **108** (2 equivalent) and **109** (2.4 equivalent) (Fig. 6A). Moreover, we envisioned that this two-step one-pot protocol may provide us with a simplified access to phosphonates with the 1,3,2-dioxaphosphinane 2-oxide motif of the calcium channel blocker efonidipine[20] (Fig. 1A). To this end, we synthesized structurally related phosphonates **111–113** in yields ranging from 58 to 99% using the two-step, one-pot protocol, with all reactions starting from 2,2-dimethylpropane-1,3-diol (**110**, 2 equivalent) and **108** (2 equivalent).

Lastly, we examined whether the micellar C(sp$^2$)–P cross-coupling can be used in other multistep one-pot procedures. Tandem processes are commonly implemented in micellar reactions in water, significantly increasing mass balance and reducing waste, cost and labor, so they are highly attractive, particularly under process chemistry settings (*e.g.*, pharmaceutical synthesis). To demonstrate the feasibility of micellar C(sp$^2$)–P cross-coupling in tandem procedures, we performed three multistep, one-pot reactions (Fig. 6B–D): (i) $S_NAr$ reaction of **114** with 4-iodoaniline followed by C(sp$^2$)–P cross-coupling with **3**, (ii) amide-bond coupling between amine **126** and benzoyl chloride followed by C(sp$^2$)–P cross-coupling with **3**, and (iii) $S_NAr$ reaction of **119** with **120**, followed by nitro group reduction, subsequent amine acylation and, finally, C(sp$^2$)–P cross-coupling with **3**. The two-step, one-pot reactions afforded the corresponding phosphonates **64** and **118** in 64 and 78% yield, respectively, and the four-step, one-pot reaction yielded phosphonate **125** in 69% (91% average yield per step), while skipping the work-up and product isolation of most of the reaction steps. These results highlight low barriers to adopting micellar C(sp$^2$)–P cross-coupling reactions in tandem processes in water.

### Cross-coupling of aryl triflates

Aryl triflates stand out as potential coupling partners for their excellent accessibility from ubiquitous phenols. However, their C–O bond is stronger than the C–I bond in aryl iodides, which may hamper cross-coupling by increasing energy barriers to oxidative addition. Moreover, the literature on cross-coupling chemistry of aryl triflates under micellar conditions is rather scarce.[72] Despite these caveats, we tested the feasibility of C(sp$^2$)–P cross-coupling of aryl triflates under micellar conditions in water, but many of our initial experiments failed, including *multimetallic* and *dual-ligand* conditions. Nevertheless, by screening various reaction conditions (see ESI†), we found that the dppf ligand promotes the cross-coupling of aryl triflates with **3** under modified *multimetallic* conditions, albeit in mediocre yields (Fig. 7). Thus, we established a small substrate scope and prepared two quinoline phosphonates **126** and **127** in 77 and 66% yield, respectively, and a phenyl alanine derivative **128** in 56% yield.

During our screening experiments (see ESI†), we noticed that adding salts containing weakly coordinating anions (*e.g.*, $NaPF_6$, $Mg(OTf)_2$, and $Zn(OTf)_2$) inhibit C(sp$^2$)–P cross-coupling reactions of aryl triflates. This finding is significant for $Zn(OTf)_2$ which is continuously formed from Zn and aryl triflate. Thus, triflate anions may thwart micellar C(sp$^2$)–P cross-coupling, stopping this reaction from a specific concentration.

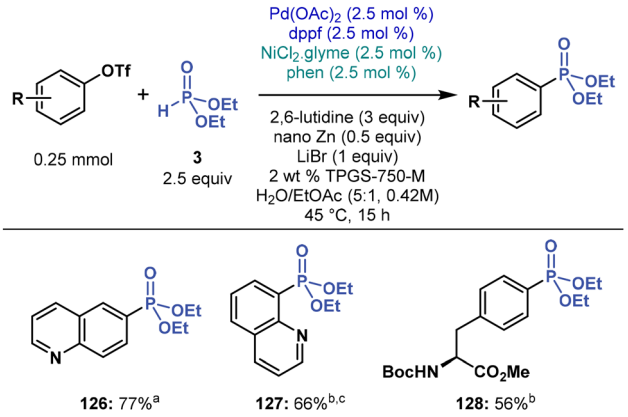


**Fig. 7** Micellar multimetallic C(sp$^2$)–P cross-coupling of aryl triflates with **3**. [a]5 mol% of $Pd(OAc)_2$, 5 mol% of dppf. [b]1 mol% $Ni(phen)_3Cl_2$. [c]Performed at 55 °C.

### Current limitations

Our method showed a broad substrate scope and functional group-tolerance. However, we encountered some limitations. In particular, *ortho*-substituted iodobenzenes bearing OH, $NH_2$, $NO_2$ and $CO_2H$ groups provided phosphonate products in poor yields (<20% by $^1$H NMR with $CH_2Br_2$ as an internal standard). Similarly, 2-iodopyridine and 2-iodopyrazine afforded no cross-coupling products. Despite affording the target products in serviceable yields (40–86%), cross-coupling reactions with some phosphorus nucleophiles (**87**, **97**, and **98**) still require further optimization to reach their full efficiency. Nevertheless, the recently reported surfactant Savie,[73] which enhances the efficiency of many transformations under micellar conditions in water, may enable us to perform C(sp$^2$)–P cross-coupling reactions at higher temperatures, at which the TPGS-750-M surfactant reaches its cloud point. These more forcing conditions may be the key to efficient cross-coupling reactions with poorly reactive (hetero)aryl halides and with strongly coordinating phosphorus nucleophiles (such as **87**, **97**, and **98**). Similarly, detailed mechanistic understanding of both *multimetallic* and *dual-ligand* reaction conditions (see ESI† for plausible mechanism) may help designing more efficient micellar C(sp$^2$)–P cross-coupling reactions and thus warrants further investigation. Our laboratory is actively pursuing these lines of research.

### Future perspectives

Our approach may be readily adopted by organic, medicinal and process chemists to develop more efficient micellar C(sp$^2$)–P cross-coupling reactions of challenging substrates (*e.g.*, 2-halopyridines, aryl triflates) while decreasing catalyst

Open Access Article. Published on 24 October 2023. Downloaded on 12/6/2025 9:19:50 AM.
This article is licensed under a Creative Commons Attribution-NonCommercial 3.0 Unported Licence.

loading, ideally to ppm levels. Initial experiments performed using *multimetallic* (2500 ppm Pd/1000 ppm Ni) and *dual-ligand* (3500 ppm Pd) conditions showed that ppm level catalysis is indeed feasible but current conditions vary in reaction performance (see ESI†). Therefore, future efforts will certainly focus on identifying more highly active catalysts and may provide more efficient access to novel scaffolds containing phosphorus, such as tertiary phosphine oxides prepared from SPOs (*e.g.*, **98**), emerging, medically relevant compounds (anticancer drugs, *e.g.*, brigatinib).

## Conclusion

This study establishes an experimental paradigm for mild, practical, general, and environmentally responsible C(sp$^2$)–P cross-coupling under *multimetallic* Pd/Ni- and *dual-ligand* Pd-catalysed conditions, overcoming current limitations of C(sp$^2$)–P cross-coupling reactions by (1) using inexpensive, widely available Pd and Ni catalyst at lower-than-typical catalyst loadings and commercially available *H*-phosphonates, *H*-phosphinates and SPOs, (2) requiring only mild heating (45–60 °C), thereby increasing functional group-tolerance and reducing energy inputs, and (3) replacing environmentally unsustainable and harmful polar aprotic solvents (*e.g.*, DMF) with water. These reactions are easy to perform, safe and readily scalable, produce less organic waste than reactions in organic solvents (see ESI† for calculations of Process Mass Intensity, PMI, values and E factors, and their comparison with those of the literature procedures), and can be applied to synthesize over 100 (hetero)aryl phosphonates, thiophosphonates, phosphinates and phosphine oxides with a wide range of functional groups, including medically relevant substrates and drugs under late-stage functionalization settings, in addition to potentially bioactive compounds. Combined, these findings open up new opportunities for applications in medicinal chemistry and life sciences by fostering the development of environmentally friendly and mild cross-coupling reactions under micellar conditions in water, including tandem processes, while expanding the toolbox of emerging multimetallic-catalysed reactions.[46a,48,74]

## Author contributions

All authors have given approval to the final version of the manuscript. R. N. conceived the idea, designed experiments, optimized the reaction conditions, established the substrate scope, collected analytical data, and wrote the manuscript. K. K. synthesized starting compounds, helped with purification and collection of analytical data. O. B. oversaw the project and secured funding.

## Conflicts of interest

There are no conflicts to declare.

## Acknowledgements

The authors greatly acknowledge financial support from the Czech Science Foundation (Grant No. 23-05752S, O. B.) and the Charles University Research Centre program (Grant No. UNCE/SCI/014). We thank Dr Michal Urban and Dr Zdeněk Tošner for their assistance with NMR experiments, Kvetoslava Kertisová for HRMS analysis, and Stanislava Matějková for ICP analysis. We thank Dr Carlos V. Melo for editing the manuscript. We are also grateful to anonymous reviewers for their valuable inputs.

## References

1 (*a*) V. Iaroshenko, *Organophosphorus Chemistry: From Molecules to Applications*, Wiley-VCH, Weinheim, 2019; (*b*) C. M. Timperley, *Best Synthetic Methods: Organophosphorus(v) Chemistry*, Academic Press, New York, 2015; (*c*) L. D. Quin, *A Guide to Organophosphorus Chemistry*, Wiley-VCH, New York, 2000; (*d*) C. Xie, A. J. Smaligo, X.-R. Song and O. Kwon, *ACS Cent. Sci.*, 2021, **7**, 536–558; (*e*) H. Guo, Y. C. Fan, Z. Sun, Y. Wu and O. Kwon, *Chem. Rev.*, 2018, **118**, 10049–10293; (*f*) W. Tang and X. Zhang, *Chem. Rev.*, 2003, **103**, 3029–3070.

2 (*a*) S. Demkowicz, J. Rachon, M. Daśko and W. Kozak, *RSC Adv.*, 2016, **6**, 7101–7112; (*b*) H. Yu, H. Yang, E. Shi and W. Tang, *Med. Drug Discovery*, 2020, **8**, 100063.

3 J. B. Rodrigueza and C. Gallo-Rodriguez, *ChemMedChem*, 2018, **14**, 190–216.

4 For example: (*a*) E. Schönbrunn, S. Eschenburg, W. A. Shuttleworth, J. V. Schloss, N. Amrhein, J. N. Evans and W. Kabsch, *Proc. Natl. Acad. Sci. U. S. A.*, 2001, **98**, 1376–1380; (*b*) C. Zhou, X. Luo, N. Chen, L. Zhang and J. Gao, *J. Agric. Food Chem.*, 2020, **68**, 3344–3353.

5 (*a*) C. Queffélec, M. Petit, P. Janvier, D. A. Knight and B. Bujoli, *Chem. Rev.*, 2012, **112**, 3777–3807; (*b*) T. Baumgartner and R. Réau, *Chem. Rev.*, 2006, **106**, 4681–4727; (*c*) T. Baumgartner, *Acc. Chem. Res.*, 2014, **47**, 1613–1622.

6 M. M. Velencoso, A. Battig, J. C. Markwart, B. Schartel and F. R. Wurm, *Angew. Chem., Int. Ed.*, 2018, **57**, 10450–10467.

7 M. V. Stambirskyi, T. Kostiuk, S. I. Sirobaba, A. Rudnichenko, D. L. Titikaiev, Y. V. Dmytriv, H. Kuznietsova, I. Pishel, P. Borysko and P. K. Mykhailiuk, *J. Org. Chem.*, 2021, **86**, 12783–12801.

8 P. Finkbeiner, J. P. Hehn and C. Gnamm, *J. Med. Chem.*, 2020, **63**, 7081–7107.

9 J. J. Marineau, K. B. Hamman, S. Hu, S. Alnemy, J. Mihalich, A. Kabro, K. M. Whitmore, D. K. Winter, S. Roy, S. Ciblat, N. Ke, A. Savinainen, A. Wilsily, G. Malojcic, R. Zahler, D. Schmidt, M. J. Bradley, N. J. Waters and C. Chuaqui, *J. Med. Chem.*, 2022, **65**, 1458–1480.

10 (*a*) G. P. Horsman and D. L. Zechel, *Chem. Rev.*, 2017, **117**, 5704–5783; (*b*) R. Engel, *Chem. Rev.*, 1977, **77**, 349–367.

Open Access Article. Published on 24 October 2023. Downloaded on 12/6/2025 9:19:50 AM.
This article is licensed under a Creative Commons Attribution-NonCommercial 3.0 Unported Licence.

11 E. D. Clercq and A. Holý, *Nat. Rev. Drug Discovery*, 2005, **4**, 928–940.

12 For example: (*a*) D. L. Higgins, R. Chang, D. V. Debabov, J. Leung, T. Wu, K. M. Krause, E. Sandvik, J. M. Hubbard, K. Kaniga, D. E. Schmidt, Q. Gao, R. T. Cass, D. E. Karr, B. M. Benton and P. P. Humphrey, *Antimicrob. Agents Chemother.*, 2005, **49**, 1127–1134; (*b*) Y. Cao, Q. Peng, S. Li, Z. Deng and J. Gao, *RSC Adv.*, 2019, **9**, 42204–42218.

13 (*a*) M. Krečmerová, P. Majer, R. Rais and B. S. Slusher, *Front. Chem.*, 2022, **10**, 889737; (*b*) K. M. Heidel and C. Dowd, *Future Med. Chem.*, 2019, **11**, 1625–1643.

14 (*a*) T. S. Elliott, A. Slowey, Y. Ye and S. J. Conway, *MedChemComm*, 2012, **3**, 735–751; (*b*) Y. Mehellou, H. S. Rattan and J. Balzarini, *J. Med. Chem.*, 2018, **61**, 2211–2226.

15 A. Mucha, P. Kafarski and Ł. Berlicki, *J. Med. Chem.*, 2011, **54**, 5955–5980.

16 (*a*) I. V. L. Wilkinson, K. J. Perkins, H. Dugdale, L. Moir, A. Vuorinen, M. Chatzopoulou, S. E. Squire, S. Monecke, A. Lomow, M. Geese, P. D. Charles, P. Burch, J. M. Tinsley, G. Wynne, S. G. Davies, F. X. Wilson, F. Rastinejad, S. Mohammed, K. E. Davies and A. J. Russell, *Angew. Chem., Int. Ed.*, 2020, **59**, 2420–2428; (*b*) M. Chatzopoulou, E. Emer, C. Lecci, J. A. Rowley, A.-S. Casagrande, L. Moir, S. E. Squire, S. G. Davies, S. Harriman, G. M. Wynne, F. X. Wilson, K. E. Davies and A. J. Russell, *ACS Med. Chem. Lett.*, 2020, **11**, 2421–2427.

17 M. D. Sørensen, L. K. A. Blæhr, M. K. Christensen, T. Høyer, S. Latini, P.-J. V. Hjarnaa and F. Björkling, *Bioorg. Med. Chem.*, 2003, **11**, 5461–5484.

18 G. Németh, Z. Greff, A. Sipos, Z. Varga, R. Székely, M. Sebestyén, Z. Jászay, S. Béni, Z. Nemes, J.-L. Pirat, J.-N. Volle, D. Virieux, Á. Gyuris, K. Kelemenics, É. Áy, J. Minarovits, S. Szathmary, G. Kéri and L. Őrfi, *J. Med. Chem.*, 2014, **57**, 3939–3965.

19 C. Dousson, F. Alexandre, A. Amador, S. Bonaric, S. Bot, C. Caillet, T. Convard, D. da Costa, M. Lioure, A. Roland, E. Rosinovsky, S. Maldonado, C. Parsy, C. Trochet, R. Storer, A. Stewart, J. Wang, B. A. Mayes, C. Musiu, B. Poddesu, L. Vargiu, M. Liuzzi, A. Moussa, J. Jakubik, L. Hubbard, M. Seifer and D. Standring, *J. Med. Chem.*, 2016, **59**, 1891–1898.

20 H. Tanaka and K. Shigenobu, *Cardiovasc. Drug Rev.*, 2002, **20**, 81–92.

21 X. Chen, D. J. Kopecky, J. Mihalic, S. Jeffries, X. Min, J. Heath, J. Deignan, S. Lai, Z. Fu, C. Guimaraes, S. Shen, S. Li, S. Johnstone, S. Thibault, H. Xu, M. Cardozo, W. Shen, N. Walker, F. Kayser and Z. Wang, *J. Med. Chem.*, 2012, **55**, 3837–3851.

22 (*a*) W. Huang, S. Liu, D. Zou, M. Thomas, Y. Wang, T. Zhou, J. Romero, A. Kohlmann, F. Li, J. Qi, L. Cai, T. A. Dwight, Y. Xu, R. Xu, R. Dodd, A. Toms, L. Parillon, X. Lu, R. Anjum, S. Zhang, F. Wang, J. Keats, S. D. Wardwell, Y. Ning, Q. Xu, L. E. Moran, Q. K. Mohemmad, H. G. Jang, T. Clackson, N. I. Narasimhan, V. M. Rivera, X. Zhu, D. Dalgarno and W. C. Shakespeare, *J. Med. Chem.*, 2016, **59**, 4948–4964; (*b*) S. Li, T. Zhang, S.-J. Zhu, C. Lei, M. Lai, L. Peng, L. Tong, Z. Pang, X. Lu and J. Ding, *ACS Med. Chem. Lett.*, 2022, **13**, 196–202.

23 (*a*) T. Hirao, T. Masunaga, Y. Ohshiro and T. Agawa, *Synthesis*, 1981, 56–57; (*b*) T. Hirao, T. Maunaga, N. Yamada, Y. Ohshiro and T. Agawa, *Bull. Chem. Soc. Jpn.*, 1982, **55**, 909–913; (*c*) M. Kalek and J. Stawinski, *Organometallics*, 2007, **26**, 5840–5847; (*d*) M. Kalek and J. Stawinski, *Organometallics*, 2008, **27**, 5876–5888; (*e*) M. Kalek, M. Jezowska and J. Stawinski, *Adv. Synth. Catal.*, 2009, **351**, 3207–3216; (*f*) E. L. Deal, C. Petit and J.-L. Montchamp, *Org. Lett.*, 2011, **13**, 3270–3273; (*g*) O. Berger, C. Petit, E. L. Deal and J.-L. Montchamp, *Adv. Synth. Catal.*, 2013, **355**, 1361–1373; (*h*) M. Kalek, A. Ziadi and J. Stawinski, *Org. Lett.*, 2008, **10**, 4637–4640; (*i*) Q. Dai, W. Li, Z. Li and J. Zhang, *J. Am. Chem. Soc.*, 2019, **141**, 20556–20564; (*j*) J. R. Moncarz, N. F. Laritcheva and D. S. Glueck, *J. Am. Chem. Soc.*, 2002, **124**, 13356–13357.

24 (*a*) D. Zhu, S. Jiang, Q. Wu, H. Wang, L. Chai, H. Li and H. Li, *Org. Lett.*, 2021, **23**, 160–165; (*b*) Y. Bai, N. Liu, S. Wang, S. Wang, S. Ning, L. Shi, L. Cui, Z. Zhang and J. Xiang, *Org. Lett.*, 2019, **21**, 6835–6838; (*c*) Y.-L. Zhao, G.-J. Wu, Y. Li, L.-X. Gao and F.-S. Han, *Chem. – Eur. J.*, 2012, **18**, 9622–9627; (*d*) C. Shen, G. Yang and W. Zhang, *Org. Biomol. Chem.*, 2012, **10**, 3500–3505.

25 (*a*) D. Gelman, L. Jiang and S. L. Buchwald, *Org. Lett.*, 2003, **5**, 2315–2318; (*b*) C. Huang, X. Tang, H. Fu, Y. Jiang and Y. Zhao, *J. Org. Chem.*, 2006, **71**, 5020–5022; (*c*) H. Zhang, X. Y. Zhang, D. Q. Dong and Z. Wang, *RSC Adv.*, 2015, **5**, 52824–52831; (*d*) R. Beaud, R. J. Phipps and M. J. Gaunt, *J. Am. Chem. Soc.*, 2016, **138**, 13183–13186.

26 (*a*) A. L. Schwan, *Chem. Soc. Rev.*, 2004, **33**, 218–224; (*b*) F. M. Tappe, V. T. Trepohl and M. Oestreich, *Synthesis*, 2010, 3037–3062; (*c*) C. S. Demmer, N. Krogsgaard-Larsen and L. Bunch, *Chem. Rev.*, 2011, **111**, 7981–8006; (*d*) U. S. Kanchana, E. J. Diana, T. V. Mathew and G. Anilkumar, *ChemistrySelect*, 2021, **6**, 1579–1588.

27 For example, please refer to: (*a*) J. Yang, T. Chen and L.-B. Han, *J. Am. Chem. Soc.*, 2015, **137**, 1782–1785; (*b*) W. C. Fu, C. M. So and F. Y. Kwong, *Org. Lett.*, 2015, **17**, 5906–5909; (*c*) H. McErlain, L. M. Riley and A. Sutherland, *J. Org. Chem.*, 2021, **86**, 17036–17049; (*d*) L. Liao, Y. Gui, X. Zhang, G. Shen, H. Liu, W. Zhou, J. Li and D. Yu, *Org. Lett.*, 2017, **19**, 3735–3738.

28 C.-G. Feng, M. Ye, K.-J. Xiao, S. Li and J.-Q. Yu, *J. Am. Chem. Soc.*, 2013, **135**, 9322–9325.

29 (*a*) C. Li, T. Yano, N. Ishida and M. Murakami, *Angew. Chem., Int. Ed.*, 2013, **52**, 9801–9804; (*b*) M. Min, D. Kang, S. Jung and S. Hong, *Adv. Synth. Catal.*, 2016, **358**, 1296–1301; (*c*) B. Li, M. Liu, S. U. Rehman and C. Li, *J. Am. Chem. Soc.*, 2022, **144**, 2893–2898.

30 J.-L. Montchamp and Y. R. Dumond, *J. Am. Chem. Soc.*, 2001, **123**, 510–511.

31 For example, please refer to: (*a*) S. K. Boyer, J. Bach, J. McKenna and E. Jagdmann Jr., *J. Org. Chem.*, 1985, **50**,

Open Access Article. Published on 24 October 2023. Downloaded on 12/6/2025 9:19:50 AM.
This article is licensed under a Creative Commons Attribution-NonCommercial 3.0 Unported Licence.

3408–3411. For reviews, refer to: (*b*) G. Brieger and T. J. Nestrick, *Chem. Rev.*, 1974, **74**, 567–580; (*c*) R. A. W. Johnstone and A. H. Wilby, *Chem. Rev.*, 1985, **85**, 129–170.

32 Y. Belabassi, S. Alzghari and J.-L. Montchamp, *J. Organomet. Chem.*, 2008, **693**, 3171–3178.

33 (*a*) C. M. Alder, J. D. Hayler, R. K. Henderson, A. M. Redman, L. Shukla, L. E. Shuster and H. F. Sneddon, *Green Chem.*, 2016, **18**, 3879–3890; (*b*) D. Prat, J. Haylerb and A. A. Wells, *Green Chem.*, 2014, **16**, 4546–4551.

34 EUR-Lex (official website of European Union law) **https://data.europa.eu/eli/reg/2021/2030/oj** (accessed July 2023).

35 (*a*) T. Kitanosono, K. Masuda, P. Xu and S. Kobayashi, *Chem. Rev.*, 2018, **118**, 679–746; (*b*) M.-O. Simon and C.-J. Li, *Chem. Soc. Rev.*, 2012, **41**, 1415–1427.

36 A. L. Casalnuovo and J. C. Calabrese, *J. Am. Chem. Soc.*, 1990, **112**, 4324–4330.

37 K. Xu, F. Yang, G. Zhang and Y. Wu, *Green Chem.*, 2013, **15**, 1055–1060.

38 S. M. Rummelt, M. Ranocchiari and J. A. van Bokhoven, *Org. Lett.*, 2012, **14**, 2188–2190.

39 X. Zhang, H. Liu, X. Hu, G. Tang, J. Zhu and Y. Zhao, *Org. Lett.*, 2011, **13**, 3478–3481.

40 For reviews, please refer to: (*a*) B. H. Lipshutz, *J. Org. Chem.*, 2017, **82**, 2806–2816; (*b*) T. Dwars, E. Paetzold and G. Oehme, *Angew. Chem., Int. Ed.*, 2005, **44**, 7174–7199; (*c*) B. H. Lipshutz, S. Ghorai and M. Cortes-Clerget, *Chem. – Eur. J.*, 2018, **24**, 6672–6695; (*d*) M. Cortes-Clerget, J. Yu, J. R. A. Kincaid, P. Walde, F. Gallou and B. H. Lipshutz, *Chem. Sci.*, 2021, **12**, 4237–4266.

41 T. Ansari, F. Gallou and S. Handa, *Coord. Chem. Rev.*, 2023, **488**, 215158.

42 For example, please refer to: (*a*) A. Krasovskiy, C. Duplais and B. H. Lipshutz, *J. Am. Chem. Soc.*, 2009, **131**, 15592–15593; (*b*) S. Handa, Y. Wang, F. Gallou and B. H. Lipshutz, *Science*, 2015, **349**, 1087–1091; (*c*) H. Pang, Y. Wang, F. Gallou and B. H. Lipshutz, *J. Am. Chem. Soc.*, 2019, **141**, 17117–17124; (*d*) H. Pang, Y. Hu, J. Yu, F. Gallou and B. H. Lipshutz, *J. Am. Chem. Soc.*, 2021, **143**, 3373–3382; (*e*) Y. Hu, X. Li, G. Jin and B. H. Lipshutz, *ACS Catal.*, 2023, **13**, 3179–3186.

43 (*a*) S. Hazra, F. Gallou and S. Handa, *ACS Sustainable Chem. Eng.*, 2022, **10**, 5299–5306; (*b*) C. M. Gabriel, M. Keener, F. Gallou and B. H. Lipshutz, *Org. Lett.*, 2015, **17**, 3968–3971.

44 (*a*) N. A. Isley, R. T. H. Linstadt, S. M. Kelly, F. Gallou and B. H. Lipshutz, *Org. Lett.*, 2015, **17**, 4734–4737; (*b*) N. R. Lee, F. Gallou and B. H. Lipshutz, *Org. Process Res. Dev.*, 2017, **21**, 218–221.

45 B. H. Lipshutz, S. Ghorai, A. R. Abela, R. Moser, T. Nishikata, C. Duplais, A. Krasovskiy, R. D. Gaston and R. C. Gadwood, *J. Org. Chem.*, 2011, **76**, 4379–4391.

46 For example, please refer to: (*a*) K. Kang, N. L. Loud, T. A. DiBenedetto and D. J. Weix, *J. Am. Chem. Soc.*, 2021, **143**, 21484–21491; (*b*) I. J. S. Fairlamb, R. J. K. Taylor, J. L. Serrano and G. Sanchez, *New J. Chem.*, 2006, **30**, 1695–1704.

47 V. T. Tran, Z.-Q. Li, O. Apolinar, J. Derosa, M. V. Joannou, S. R. Wisniewski, M. D. Eastgate and K. M. Engle, *Angew. Chem., Int. Ed.*, 2020, **59**, 7409–7413.

48 A. M. Olivares and D. J. Weix, *J. Am. Chem. Soc.*, 2018, **140**, 2446–2449.

49 C. M. Gabriel, N. R. Lee, F. Bigorne, P. Klumphu, M. Parmentier, F. Gallou and B. H. Lipshutz, *Org. Lett.*, 2017, **19**, 194–197.

50 B.p. of **3** is 187–188 °C and b.p. of 2,6-lutidine is 143–145 °C (both at atmospheric pressure).

51 For example, please refer to: (*a*) G. Meng, Z. Wang, H. S. S. Chan, N. Chekshin, Z. Li, P. Wang and J.-Q. Yu, *J. Am. Chem. Soc.*, 2023, **145**, 8198–8208; (*b*) S. K. Sinha, S. Panja, J. Grover, P. S. Hazra, S. Pandit, Y. Bairagi and X. L. Zhang, *J. Am. Chem. Soc.*, 2022, **144**, 12032–12042; (*c*) D. Zhao, P. Xu and T. Ritter, *Chem*, 2019, **5**, 97–107; (*d*) H. Chen, P. Wedi and T. Meyer, *Angew. Chem., Int. Ed.*, 2018, **57**, 2497–2501.

52 W. M. Cheng, R. Shang and Y. Fu, *Nat. Commun.*, 2018, **9**, 5215.

53 B. Zhao, R. Shang, G.-Z. Wang, S. Wang, H. Chen and Y. Fu, *ACS Catal.*, 2020, **10**, 1334–1343.

54 P. W. N. M. van Leeuwen, P. C. J. Kamer, J. N. H. Reek and P. Dierkes, *Chem. Rev.*, 2000, **100**, 2741–2769.

55 The following study showed that high-bite angle diphosphine ligands induce rapid C($sp^2$)–P bond-forming reductive limination: M. C. Kohler, T. V. Grimes, X. Wang, T. R. Cundari and R. A. Stockland Jr., *Organometallics*, 2009, **28**, 1193–1201.

56 (*a*) M.-N. Birkholz, Z. Freixa and P. W. N. M. van Leeuwen, *Chem. Soc. Rev.*, 2009, **38**, 1099–1118; (*b*) P. W. N. M. van Leeuwen and P. C. J. Kamer, *Catal. Sci. Technol.*, 2017, **8**, 26–113.

57 (*a*) P. A. Cox, M. Reid, A. G. Leach, A. D. Campbell, E. J. King and G. C. Lloyd-Jones, *J. Am. Chem. Soc.*, 2017, **139**, 13156–13165; (*b*) L. Chen, D. R. Sanchez, B. Zhang and B. P. Carrow, *J. Am. Chem. Soc.*, 2017, **139**, 12418–12421.

58 P. J. Medina and S. Goodin, *Clin. Ther.*, 2008, **30**, 1426–1447.

59 B. G. Janesko, H. C. Fisher, M. J. Bridle and J.-L. Montchamp, *J. Org. Chem.*, 2015, **80**, 10025–10032.

60 G. Manca, M. Caporali, A. Ienco, M. Peruzzini and C. Mealli, *J. Organomet. Chem.*, 2014, **760**, 177–185.

61 K. D. Troev, *Reactivity of P–H Group of Phosphorus Based Compounds*, Elsevier, London, 2017, and references therein.

62 U. Pradere, E. C. Garnier-Amblard, S. J. Coats, F. Amblard and R. F. Schinazi, *Chem. Rev.*, 2014, **114**, 9154–9218, and references therein.

63 M. Békés, D. R. Langley and C. M. Crews, *Nat. Rev. Drug Discovery*, 2022, **21**, 181–200.

64 For example, please refer to: (*a*) C. P. Tam, L. Zhou, A. C. Fahrenbach, W. Zhang, T. Walton and J. W. Szostak, *J. Am. Chem. Soc.*, 2018, **140**, 783–792; (*b*) W. Zhang, C. P. Tam, J. Wang and J. W. Szostak, *ACS Cent. Sci.*, 2016, **2**, 916–926.

65 T. Johansson and J. Stawinski, *Tetrahedron*, 2004, **60**, 389–395.

Open Access Article. Published on 24 October 2023. Downloaded on 12/6/2025 9:19:50 AM.
This article is licensed under a Creative Commons Attribution-NonCommercial 3.0 Unported Licence.

66 (*a*) T. M. Shaikh, C.-M. Weng and F.-E. Hong, *Coord. Chem. Rev.*, 2012, **256**, 771–803; (*b*) P. Sutra and A. Igau, *Coord. Chem. Rev.*, 2016, **308**, 97–116.

67 For example, please refer to: (*a*) A. Gernet, N. Sevrain, J. N. Volle, T. Ayad, J. L. Pirat and D. Virieux, *J. Org. Chem.*, 2020, **85**, 14730–14743; (*b*) H. Rao, Y. Jin, H. Fu, Y. Jiang and Y. Zhao, *Chem. – Eur. J.*, 2006, **12**, 3636–3646; (*c*) M. Toffano, C. Dobrota and J.-C. Fiaud, *Eur. J. Org. Chem.*, 2006, 650–656; (*d*) Y. Xu, J. Xia and H. Guo, *Synthesis*, 1986, 691–692.

68 M. Oba, K. Kojima, M. Endo, H. Sano and K. Nishiyama, *Green Chem. Lett. Rev.*, 2013, **6**, 233–236.

69 J.-L. Montchamp, *Acc. Chem. Res.*, 2014, **47**, 77–87, and references therein.

70 T. M. Lord, S. L. Casino, S. E. Hartzell, K. J. Garcia, R. D. Pike and R. A. Stockland Jr., *ChemistrySelect*, 2016, **1**, 2188–2191.

71 (*a*) A. D. Dal-Maso, F. Legendre, C. Blonski and P. Hoffmann, *Synth. Commun.*, 2008, **38**, 1688–1693; (*b*) Q. Xiao, Y. Ju and Y. Zhao, *Heteroat. Chem.*, 2003, **14**, 208–210.

72 A few examples can be found in: (*a*) S. Handa, E. D. Slack and B. H. Lipshutz, *Angew. Chem., Int. Ed.*, 2015, **54**, 11994–11998; (*b*) E. B. Landstrom, N. Akporji, N. R. Lee, C. M. Gabriel, F. C. Braga and B. H. Lipshutz, *Org. Lett.*, 2020, **22**, 6543–6546; (*c*) S. Handa, F. Ibrahim, T. N. Ansari and F. Gallou, *ChemCatChem*, 2018, **10**, 4229–4233.

73 J. R. A. Kincaid, M. J. Wong, N. Akporji, F. Gallou, D. M. Fialho and B. H. Lipshutz, *J. Am. Chem. Soc.*, 2023, **145**, 4266–4278.

74 (*a*) L. K. G. Ackerman-Biegasiewicz, S. K. Kariofillis and D. J. Weix, *J. Am. Chem. Soc.*, 2023, **145**, 6596–6614; (*b*) L. K. G. Ackerman, M. M. Lovell and D. J. Weix, *Nature*, 2015, **524**, 454–457.

 This journal is © The Royal Society of Chemistry 2023